



THE UNIVERSITY *of* EDINBURGH

Edinburgh Research Explorer

## A deep root for the Cambrian Explosion: implications of new bio- and chemostratigraphy from the Siberian Platform

**Citation for published version:**

Zhu, M, Zhuravlev, A, Wood, R, Zhao, F & Sokhov, S 2017, 'A deep root for the Cambrian Explosion: implications of new bio- and chemostratigraphy from the Siberian Platform', *Geology*, vol. 45, no. 5, pp. 459-462. <https://doi.org/10.1130/G38865.1>

**Digital Object Identifier (DOI):**

[10.1130/G38865.1](https://doi.org/10.1130/G38865.1)

**Link:**

[Link to publication record in Edinburgh Research Explorer](#)

**Document Version:**

Peer reviewed version

**Published In:**

Geology

**Publisher Rights Statement:**

© Geological Society of America

**General rights**

Copyright for the publications made accessible via the Edinburgh Research Explorer is retained by the author(s) and / or other copyright owners and it is a condition of accessing these publications that users recognise and abide by the legal requirements associated with these rights.

**Take down policy**

The University of Edinburgh has made every reasonable effort to ensure that Edinburgh Research Explorer content complies with UK legislation. If you believe that the public display of this file breaches copyright please contact [openaccess@ed.ac.uk](mailto:openaccess@ed.ac.uk) providing details, and we will remove access to the work immediately and investigate your claim.



# Geology

## A deep root for the Cambrian Explosion: implications of new bio- and chemostratigraphy from the Siberian Platform

--Manuscript Draft--

<b>Manuscript Number:</b>	G38865R1
<b>Full Title:</b>	A deep root for the Cambrian Explosion: implications of new bio- and chemostratigraphy from the Siberian Platform
<b>Short Title:</b>	A deep root for the Cambrian Explosion
<b>Article Type:</b>	Article
<b>Keywords:</b>	Ediacaran; Cambrian Explosion; chemostratigraphy; biostratigraphy; small shelly fossils; carbon isotope excursion; Siberia.
<b>Corresponding Author:</b>	Mao-yan Zhu Nanjing Institute of Geology and Palaeontology, Chinese Academy of Sciences Nanjing, Jiangsu CHINA
<b>Corresponding Author Secondary Information:</b>	
<b>Corresponding Author's Institution:</b>	Nanjing Institute of Geology and Palaeontology, Chinese Academy of Sciences
<b>Corresponding Author's Secondary Institution:</b>	
<b>First Author:</b>	Mao-yan Zhu
<b>First Author Secondary Information:</b>	
<b>Order of Authors:</b>	Mao-yan Zhu Andrey Zhuravlev Rachel Wood Fangchen Zhao Sergey Sokhov
<b>Order of Authors Secondary Information:</b>	
<b>Manuscript Region of Origin:</b>	RUSSIAN FEDERATION
<b>Abstract:</b>	<p>Much uncertainty remains as to the temporal relationship between the Ediacaran and Cambrian biotas, yet this is critical to our understanding of the rise of metazoans. Here we present new high resolution carbon isotope chemostratigraphy and biostratigraphy for a terminal Ediacaran to Cambrian succession on the eastern Siberian Platform, Russia, which shows the presence of a succession of diverse fossil assemblages before the start of the basal Cambrian negative carbon isotope excursion (BACE). Soft-bodied Ediacaran biota (<i>Beltanelliformis</i>) occur before the start of the late Ediacaran positive carbon isotope plateau (EPIP), a mixed Ediacaran and Cambrian skeletal biota (<i>Cloudina</i>, <i>Anabarites</i>, <i>Cambrotubulus</i>) appear within the EPIP, and diverse Cambrian-type small shelly fossils including <i>Protohertzina</i> and other protocondonts, halkieriids, chancelloriids, hyoliths, hyolithelminthes and the burrowing trace fossil (<i>Diplocraterion</i>) appear at the beginning of the BACE. These integrated data show that taxa attributed to so-called Ediacaran and earliest Cambrian skeletal biotas in fact overlap without notable biotic turnover, and thus refute the presence of a large isotope excursion coincident with mass extinction of all Ediacaran biota. We propose a new biozone, the <i>Cloudina-Namacalathus-Sinotubulites</i> Assemblage Zone, to precede the known small shelly fossil (SSF) zones. These observations raise doubts as to whether there is any true separation between the Ediacaran and Cambrian skeletal biotas, and suggest that there is a deep root for the Cambrian Explosion of metazoans.</p>
<b>Response to Reviewers:</b>	Many thanks for support from three reviewers that our work will be an excellent contribution to GEOLOGY, and their helpful comments and corrections on our manuscript. We considered the comments carefully and made necessary revisions and

corrections in text and figures. Major changes and responses to reviewers' comments are listed here, you will find more detail responses to reviews as attached file.

1. The main argument of the reviews (particularly from Reviewer #2) is the age model of the Ust'-Yudoma Formation. The key point is that whether the negative excursion between the Aim and Ust'-Yudoma formations could be the BACE. In fact, a late Ediacaran age for the Ust'-Yudoma formations is not just based on the occurrence of Cloudina, but also based on the integrated correlations from the bio-, chemostratigraphy and sequence stratigraphy of entire Yudoma Group and overlying Pestrotsvet Formation, and their global correlations as stated in detail in the "Discussion". The negative excursions below the Ust'-Yudoma Formation may be of local or regional significance within the terminal Ediacaran carbon isotope plateau, as this is also reported from the equivalent terminal Ediacaran Khatyspyt Formation in NE Siberia (Cui et al., 2016, PPP, 461:122-139). Similar to the Aim Formation, the Khatyspyt Formation also consists of a black limestone with abundant characteristic soft-bodied Ediacara fossils, thus both are a late Ediacaran age below the BACE. Since we resent a short paper, there is no space to add more detailed discussion on the age model for whole sequence and its global correlation. But as Reviewer #1 has pointed out there are no data to suggest a Cambrian age for the Ust'-Yudoma Formation. Reviewer # 3 (Dr. Huan Cui), who has been working on late Ediacaran stratigraphy both in Siberia and South China, indeed has no issue with the proposed age model. But in order to make the point more clearly, we revised relevant part in the "Discussion" and added one new reference (Line 121-142).

2. All three figures were revised in order to meet reviews and size limit.

a. Figure 1: We added the unconformity above the Ust'-Yudoma Formation, and replaced symbols on the map.

b. Figure 2: We added two more images of Cloudina as requested by Reviewer # 2, and one image of Shaanxilites as requested by Reviewer # 1. Meanwhile, we deleted few images to reduce the size for saving space for text. Subsequent citations in the text and caption in revised.

c. Figure 3: Revised the font size in order to meet publication.

3. Because of page limit, the text was condensed and the references were updated. The text was shortened by ca. 940 characters, together with the reduced size of Figure 2, it should meet the four page limit. If printing format is 2 columns as Figure 1 and 3 were prepared with Figure 2 for full page width, I think it would meet page limit.

1 A deep root for the Cambrian Explosion: Implications of  
2 new bio- and chemostratigraphy from the Siberian Platform

3 M. Zhu<sup>1,2\*</sup>, A. Yu. Zhuravlev<sup>3</sup>, R.A. Wood<sup>4</sup>, F. Zhao<sup>1</sup>, and S.S. Sukhov<sup>5</sup>

4 <sup>1</sup>*State Key Laboratory of Palaeobiology and Stratigraphy, Nanjing Institute of Geology  
5 and Palaeontology, Nanjing 210008, China*

6 <sup>2</sup>*College of Earth Sciences, University of Chinese Academy of Sciences, Beijing 100049,  
7 China*

8 <sup>3</sup>*Department of Biological Evolution, Faculty of Biology, Lomonosov Moscow State  
9 University, Leninskie gory 1(12), Moscow 119234, Russia*

10 <sup>4</sup>*School of GeoSciences, University of Edinburgh, James Hutton Road, Edinburgh EH9  
11 3FE, UK*

12 <sup>5</sup>*Siberian Scientific Research Institute of Geology, Geophysics and Mineral Resources,  
13 Krasny prospekt 67, Novosibirsk 630091, Russia*

14 \*E-mail address: myzhu@nigpas.ac.cn

15 **ABSTRACT**

16 Much uncertainty remains as to the temporal relationship between the Ediacaran  
17 and Cambrian biotas, yet this is critical to our understanding of the rise of metazoans.  
18 Here we present new high resolution carbon isotope chemostratigraphy and  
19 biostratigraphy for a terminal Ediacaran to Cambrian succession on the eastern Siberian  
20 Platform, Russia, which shows the presence of a succession of diverse fossil assemblages  
21 before the start of the basal Cambrian negative carbon isotope excursion (BACE). Soft-  
22 bodied Ediacaran biota (*Beltanelliformis*) occur before the start of the late Ediacaran

23 positive carbon isotope plateau (EPIP), a mixed Ediacaran and Cambrian skeletal biota  
24 (*Cloudina*, *Anabarities*, *Cambrotubulus*) appear within the EPIP, and diverse Cambrian-  
25 type small shelly fossils including *Protohertzina* and other protocondonts, halkieriids,  
26 cancelloriids, hyoliths, hyolithelminthes and the burrowing trace fossil (*Diplocraterion*)  
27 appear at the beginning of the BACE. These integrated data show that taxa attributed to  
28 so-called Ediacaran and earliest Cambrian skeletal biotas in fact overlap without notable  
29 biotic turnover, and thus refute the presence of a large isotope excursion coincident with  
30 mass extinction of all Ediacaran biota. We propose a new biozone, the *Cloudina*-  
31 *Namacalathus-Sinotubulites* Assemblage Zone, to precede the known small shelly fossil  
32 (SSF) zones. These observations raise doubts as to whether there is any true separation  
33 between the Ediacaran and Cambrian skeletal biotas, and suggest that there is a deep root  
34 for the Cambrian Explosion of metazoans.

## 35 INTRODUCTION

36 Diverse soft-bodied and skeletal macroscopic fossils first appeared in the  
37 Ediacaran (~575–541 Million years ago (Ma)) and probably represent stem- and crown-  
38 group metazoans as well as extinct clades (e.g., Droser and Gehling, 2015). This biota  
39 largely disappeared across the Precambrian-Cambrian boundary, which is thought to be  
40 marked by the ‘Great Unconformity’ and the basal Cambrian negative carbon isotope  
41 excursion (BACE) (e.g. Amthor et al., 2003; Zhu et al., 2006, 2007; Peters and Gaines,  
42 2012). This excursion pre-dates the first appearance of *Treptichnus pedum* (Zhu et al.,  
43 2001; Cui et al., 2016; Smith et al., 2016) which defines the Precambrian-Cambrian  
44 boundary (Landing, 1994), and marks a major biotic turnover as it was followed by the  
45 rapid appearance and diversification of bilaterian animals in the early Cambrian (Erwin et

46 al., 2011). The relationship between the Ediacaran and Cambrian biotas is, however,  
47 poorly known, due to the incomplete nature of most successions worldwide, taphonomic  
48 bias of fossil preservation, restriction of metazoans to oxygenated habits above an often  
49 shallow chemocline, and the difficulty of integrating commonly disparate bio- and  
50 chemostratigraphic data. Yet whether these biotas are distinct or related is fundamental to  
51 our understanding of the environmental controls on the rise of metazoans.

52 Here we present new high resolution  $\delta^{13}\text{C}$  and biostratigraphic data from a highly  
53 fossiliferous terminal Ediacaran to Cambrian succession on the distal edge of the eastern  
54 Siberian Platform, Russia. This demonstrates for the first time that there was considerable  
55 diversification of characteristic Cambrian-type skeletal taxa prior to the BACE. In turn  
56 this raises doubts as to whether there is any true separation between the Ediacaran and  
57 Cambrian skeletal biotas.

## 58 **GEOLOGICAL SETTING**

59 We consider the carbon isotope stratigraphy and fossil records at Kyra-Ytyga  
60 River, a Ediacaran-Cambrian section on the Yudoma River that formed in the Yudoma-  
61 Maya Depression on the southeastern edge of the Siberian Platform (Fig. 1A). This  
62 depression shows facies distinct from other well-known Ediacaran-Cambrian transitional  
63 successions from the Aldan, Olenek, Kotuy, and Sukharikha rivers (Khomentovsky,  
64 2008; Fig. 1A). The section encompasses the Yudoma Group which is subdivided into  
65 the Aim and Ust'-Yudoma formations (Khomentovsky, 2008) (Fig. 1B). The lower Aim  
66 Formation (~50 m) is composed of a transgressive systems tract (TST) of basal gray  
67 sandstones and red shales, and a highstand systems tract (HST) of the limey dolostones.  
68 The upper Aim Formation (~55 m) forms a second sequence and is dominated by dark

69 and finely laminated limestones with thin black shales that represent a the maximum  
70 flooding surface followed by black limestone of the HST. The Ust'-Yudoma Formation  
71 (~280 m) consists of a third thick sequence of shallow marine massive dolostones,  
72 passing transitionally into mixed dolostone and dolomitic limestone at ~180 m from the  
73 base, with laminated dolomitic limestone appearing in the final 14 m. The Ust'-Yudoma  
74 Formation ends in a regional unconformity and is overlain by the Pestrotsvet Formation  
75 in other Yudoma River sections (Khomentovsky, 2008).

## 76 CHEMOSTRATIGRAPHY

77 A near complete high resolution  $\delta^{13}\text{C}$  chemostratigraphic curve (352 data points)  
78 was constructed for ~336 m stratigraphic thickness of the Aim and Ust'-Yudoma  
79 formations (Fig. 1B; see *Supplementary Materials*). The basal dolostone of the Aim  
80 Formation has  $\delta^{13}\text{C}$  values of 0–2‰ with a short-lived negative excursion to –0.8‰  
81 occurring at 10 m, then succeeding limestone  $\delta^{13}\text{C}$  values show a stepped increase to  
82 +4‰ before a pronounced negative excursion to –1.2‰ toward the top of the formation  
83 coincident with a sequence boundary and major lithological changes. Within the  
84 dominantly dolomitic Ust'-Yudoma Formation,  $\delta^{13}\text{C}$  values rapidly increase to +2.6‰  
85 within < 10 m of the formation base, then show an extensive +1‰ to +3‰ plateau with a  
86 very stable and steady trend gradually increasing to +3‰ by 100 m up-section, then  
87 gradually decreasing to +0.5‰ by ~250 m in height from the base of the Ust'-Yudoma  
88 Formation showing a consistent fluctuation of 1‰. The final ~45 m of section shows a  
89 steady declining trend from +1.7‰ to –0.65‰.

## 90 BIOSTRATIGRAPHY

91           The continuous Kyra-Ytyga River section is characterized by five successive  
92 assemblages of fossils, Levels I to V in ascending order (Fig. 1B; See *Supplementary*  
93 *Materials*). Level I is restricted to the laminated limestone of the upper Aim Formation,  
94 and includes the Ediacaran soft-bodied *Beltanelliformis brunsa* (Fig. 2U) and  
95 ?*Shaanxilithes* (= *Nenoxites*) sp. (Wood et al., 2016; Ivantsov, 2017). Further Ediacaran  
96 fossils have been reported from the equivalent interval of the Aim Formation of proximal  
97 Yudoma River sections, including *Shaanxilithes* sp. ((Fig. 2W), *Palaeopascichnus* sp.,  
98 *Suvorovella aldanica*, and *Aspidella terranovica* (Zhuravlev et al., 2009; Wood et al.,  
99 2016; Ivantsov, 2017).

100           The first skeletal fossils appear 183 m from the base of the Ust'-Yudoma  
101 Formation (Level II), including *Cloudina* ex gr. *C. riemkeae* (Fig. 2A-C), cloudinids (Fig.  
102 2E), *Anabarites trisulcatus*, *A. valkovi* (Fig. 2F), and other undetermined SSFs (Fig. 2R)  
103 (see also Zhuravlev et al. 2012; Wood et al., 2016).

104           A small shelly fossil (SSF) assemblage appears 260 m from the base of the Ust'-  
105 Yudoma Formation (Level III), dominated by various anabaritids reaching up to 5 mm in  
106 tube length (Figs. 2S-T). These fossils are abundant and preserved either as carbonate  
107 shells or as casts within the dolostone.

108           The topmost dolomitic limestone the Ust'-Yudoma Formation is especially rich in  
109 SSFs. By 8 m below the top of the formation (Level IV), the fauna is represented by  
110 various anabaritids (Figs. 2G-I), cloudinids (Fig. 2D), and protoconodonts (Fig. 2M). The  
111 most diverse assemblage appears within the top 4.7 m of the formation (Level V),  
112 consisting of anabaritids, orthothecimorph hyoliths, protoconodonts (Figs. 2L, 2N, 2P),



113 halkieriids (Fig. 2Q), *Sachites* sp. (Fig. 2J), siphogonuchitids, cancelloriids (Fig. 2O),  
114 hyolithelminthes (Fig. 2K), and the vertical burrowing trace *Diplocraterion* sp. (Fig. 2V).

## 115 **DISCUSSION**

116       The new  $\delta^{13}\text{C}$  data provide evidence for a short interval (~50 m) of highly  
117 variable isotopic signatures, followed very protracted interval (>275 m) of very stable,  
118 positive values. This is interpreted as the late Ediacaran positive carbon isotope plateau  
119 (EPIP). Only in the final ~20 m is the start of a negative downturn of the  $\delta^{13}\text{C}$  values  
120 from 1.43 ‰ to -0.65 ‰ recorded. We interpret this to be the start of the BACE based on  
121 the following lines of evidence: (1) the continuous Ust'-Yudoma shallow marine  
122 carbonate sequence, which underwent very early dolomitization (Wood et al., 2016),  
123 shows dominantly stable  $\delta^{13}\text{C}$  values, and the start of a negative downturn in the absence  
124 of any lithological change. We suggest the  $\delta^{13}\text{C}$  data record an original seawater  
125 signature and are thus correlatable with the isotopic plateau recorded in the terminal  
126 Ediacaran sequences globally (e.g. Amthor et al., 2003; Zhu et al., 2007; Wood et al.,  
127 2015; Smith et al., 2016), (2) the sequence is below the Pestrosvet Formation  
128 unconformity, which occurs above the BACE (Khomentovsky and Karlova, 2005), and  
129 (3) a succession of overlapping Ediacaran (in particular cloudinids) and earliest Cambrian  
130 skeletal taxa are present prior to this excursion.

131       The Kyra-Ytyga succession records representative assemblages of both classic  
132 Ediacaran and Cambrian fossils. Level 1 yields *Beltanelliformis* and ?*Shaanxilithes*  
133 which represent soft-bodied Ediacaran taxa. The *Cloudina*-*Anabarites* assemblage at  
134 Levels II can be interpreted as being uppermost Ediacaran by the presence of *Cloudina*,  
135 but *Anabarites* suggests that it can also be attributed to the Nemakit-Daldynian

136 *Anabarites trisulcatus* Zone of Siberian stratigraphy. Levels III to V contain various  
137 anabariids, protoconodonts, halkieriids, chancelloriids, hyolithelminthes, hyoliths as  
138 well as vertical burrows are indicative of the *Anabarites trisulcatus* and even *Purella*  
139 *antiqua* zones, which previously only reported in the interval within or above the BACE  
140 and below the sub-Tommotian unconformity on the Siberian Platform (Khomentovsky  
141 and Karlova, 2005), and are usually considered to be typical of basal Cambrian levels  
142 globally (Steiner et al., 2007; Landing et al., 2013; Yang et al., 2016a).

143         The chemo- and biostratigraphy presented here allows correlation with other  
144 regional successions across the Ediacaran – Cambrian transition: many are either  
145 relatively condensed or contain significant unconformities (including the Great  
146 Unconformity). For example, in northwestern Canada, South China and Kazakhstan a  
147 mixed Ediacaran – Cambrian skeletal fauna characterizes the interval above the EPIP and  
148 BACE, where the earliest occurrence is close to the nadir of the isotope excursion (Pyle  
149 et al., 2006; Yang et al., 2016a). While in Nevada, USA, although both the EPIP and  
150 BACE are recorded, the Cambrian-type fossils occur only after the BACE (Smith et al.,  
151 2016). The Kyra-Ytyga section therefore provides the only documentation of both  
152 Ediacaran and Cambrian skeletal taxa within the EPIP and prior to the BACE. This may  
153 be due to the fact that Yudoma Group suffered less erosion during the formation of Great  
154 Unconformity in the area (Khomentovsky and Karlova, 2005). Additionally, the  
155 preservation of the Ediacaran skeletal fossils is limited to very shallow lithofacies above  
156 the oxic chemocline, as found at Kyra-Ytyga (Wood et al., 2016). Ediacaran successions  
157 deposited below the chemocline would be expected to lack such faunas.

158 In sum, these integrated data demonstrate that there was considerable  
159 diversification of skeletal metazoans prior to the BACE. Extrapolation of radiometric  
160 dating from the South China (Yang et al., 2016b), northern Siberian Platform (Cui et al.,  
161 2016), and Oman (Bowring et al., 2007), constrains this transitional skeletal biota to the  
162 545–540 Ma time interval.

163 The new data show that the Ediacaran and the earliest Cambrian biotas  
164 overlapped without any notable biotic turnover (Fig. 3). The BACE can now be  
165 constrained to have occurred within the interval of characteristic Cambrian-type skeletal  
166 fossil distribution (Fig. 3), thus refuting the presence of a large carbon isotope excursion  
167 coincident with the mass extinction of all Ediacaran biota. These observations in turn  
168 raise doubts as to whether there is any true separation between the Ediacaran and  
169 Cambrian skeletal biotas. Indeed, this contention is supported by the co-occurrence of  
170 cloudinids with various skeletal species representing a number of diverse clades of early  
171 Cambrian aspect in Siberia, South China, and Kazakhstan (Zhuravlev et al., 2012; Yang  
172 et al., 2016a).

173 Placing the relatively complete Kyra-Ytyga section within a global correlation  
174 scheme reveals the need to establish a new SSF biozone. We hence propose the  
175 *Cloudina-Namacalathus-Sinotubulites* Assemblage Zone based on the global and additive  
176 distribution of these three taxa (Hofmann and Mountjoy, 2001; Zhuravlev et al., 2012), to  
177 precede the well-known SSF I (*Anabarites trisulcatus*–*Protohertzina anabarica*), SSF II (  
178 = *Purella antiqua*), and SSF III (= *Watsonella crosbyi*) zones (Steiner et al., 2007; Yang  
179 et al., 2016a).

180 A notable reduction in biodiversity of the soft-bodied Ediacaran biota started at  
181 ~550 Ma, with nearly all becoming extinct at the base of the Cambrian (Laflamme et al.,  
182 2013). Due to the Great Unconformity, which was diachronous and possibly extended up  
183 to at least ~20 Myr duration in the shallow shelf area on the most paleocontinents (Fig.  
184 3), extinction of the soft bodied Ediacaran biota may in fact have been gradual rather than  
185 abrupt. To support the ‘biotic replacement’ model (Laflamme et al., 2013), however,  
186 requires further demonstration of competitive or predatory displacement. In conclusion,  
187 our new integrated data do not support the contention that extinction of the Ediacaran  
188 biota facilitated the Cambrian Explosion, but rather suggest that there is a deep root for  
189 the Cambrian Explosion of metazoans.

#### 190 **ACKNOWLEDGMENTS**

191 We thank the Director of Biological Resources and Protected Natural Territories  
192 of the Ministry of Nature Protection of the Republic of Sakha (Yakutia), led by Semen  
193 Terekhov and the administration of the Ust’-Maya Region for logistical support, and  
194 Nikolay Atlasov and Elena Aleksandrova for fieldwork support. MZ and FZ received  
195 grants support from the Ministry of Science and Technology of China (2013CB835006),  
196 the Chinese Academy of Sciences (XDB18030304), and the National Natural Science  
197 Foundation of China. We thank Aleksandr Fedorov and Andrey Ivantsov for supplying  
198 images of the fossils, Shuhai Xiao and Guoxiang Li for discussion on the fossils, and  
199 Huan Cui and other two anonymous reviewers for helpful suggestions.

#### 200 **REFERENCES CITED**

201 Amthor, J.E., Grotzinger, J.P., Schröder, S., Bowring, S.A., Ramezani, J., Martin, M.W.,  
202 and Matter, A., 2003, Extinction of *Cloudina* and *Namacalathus* at the Precambrian–

- 203 Cambrian boundary in Oman: *Geology*, v. 31, p. 431–434, doi:10.1130/0091-  
204 7613(2003)031<0431:EOCANA>2.0.CO;2.
- 205 Bowring, S., Grotzinger, J., Condon, D., Ramezani, J., Newall, M., and Allen, P., 2007,  
206 Geochronologic constraints of the chronostratigraphic framework of the  
207 Neoproterozoic Huqf Supergroup, Sultanate of Oman: *American Journal of Science*,  
208 v. 307, p. 1097–1145, doi:10.2475/10.2007.01.
- 209 Cui, H., Grazhdankin, D.V., Xiao, S., Peek, S., Rogov, V.I., Bykova, N.V., Sievers, N.E.,  
210 Liu, X.-M., and Kaufman, A.J., 2016, Redox-dependent distribution of early macro-  
211 organisms: Evidence from the terminal Ediacaran Khatyspyt Formation in Arctic  
212 Siberia: *Palaeogeography, Palaeoclimatology, Palaeoecology*, v. 461, p. 122–139,  
213 doi:10.1016/j.palaeo.2016.08.015.
- 214 Droser, M., and Gehling, J.G., 2015, The advent of animals: The view from the  
215 Ediacaran: *Proceedings of the National Academy of Sciences of the United States of*  
216 *America*, v. 112, p. 4865–4870, doi:10.1073/pnas.1403669112.
- 217 Erwin, D.H., Laflamme, M., Tweedt, S.M., Sperling, E.A., Pisani, D., and Peterson, K.J.,  
218 2011, The Cambrian conundrum: Early divergence and later ecological success in  
219 the early history of animals: *Science*, v. 334, p. 1091–1097,  
220 doi:10.1126/science.1206375.
- 221 Hofmann, H.J., and Mountjoy, E.W., 2001, *Namacalathus*—*Cloudina* assemblage in  
222 Neoproterozoic Miette Group (Byng Formation), British Columbia: Canada’s oldest  
223 shelly fossils: *Geology*, v. 29, p. 1091–1094, doi:10.1130/0091-  
224 7613(2001)029<1091:NCAINM>2.0.CO;2.

- 225 Ivantsov, A.Yu., 2017, On the finds of typical Ediacaran fossils in the Vendian Yudoma  
226 Group of eastern Siberia: *Doklady Akademii nauk*, v. 472, p. 1–4 [in Russian].
- 227 Khomentovsky, V.V., 2008, The Yudomian of Siberia, Vendian and Ediacaran systems  
228 of the International Stratigraphic Scale: *Stratigraphy and Geological Correlation*,  
229 v. 16, p. 581–598, doi:10.1134/S0869593808060014.
- 230 Khomentovsky, V.V., and Karlova, G.A., 2005, The Tommotian Stage base as the  
231 Cambrian lower boundary in Siberia: *Stratigraphy and Geological Correlation*, v. 13,  
232 p. 26–40.
- 233 Laflamme, M., Darroch, S.A.F., Tweedt, S.M., Peterson, K.J., and Erwin, D.H., 2013,  
234 The end of the Ediacara biota: Extinction, biotic replacement, or Cheshire Cat?:  
235 *Gondwana Research*, v. 23, p. 558–573, doi:10.1016/j.gr.2012.11.004.
- 236 Landing, E., 1994, Precambrian-Cambrian boundary ratified and a new perspective of  
237 Cambrian time: *Geology*, v. 22, p. 179–182, doi:10.1130/0091-  
238 7613(1994)022<0179:PCBGSR>2.3.CO;2.
- 239 Landing, E., Geyer, G., Brasier, M.D., and Bowring, S.A., 2013, Cambrian Evolutionary  
240 Radiation: Context, correlation, and chronostratigraphy—Overcoming deficiencies  
241 of the first appearance datum (FAD) concept: *Earth-Science Reviews*, v. 123,  
242 p. 133–172, doi:10.1016/j.earscirev.2013.03.008.
- 243 Peters, S.E., and Gaines, R.R., 2012, Formation of the ‘Great Unconformity’ as a trigger  
244 for the Cambrian explosion: *Nature*, v. 484, p. 363–366, doi:10.1038/nature10969.
- 245 Pyle, L.J., Narbonne, G.M., Nowlan, G.S., Xiao, S., and James, N.P., 2006, Early  
246 Cambrian metazoan eggs, embryos, and phosphatic microfossils from northwestern

- 247 Canada: *Journal of Paleontology*, v. 80, p. 811–825, doi:10.1666/0022-  
248 3360(2006)80[811:ECMEEA]2.0.CO;2.
- 249 Smith, E.F., Nelson, L.L., Strange, M.A., Eyster, A.E., Rowland, S.M., Schrag, D.P., and  
250 Macdonald, F.A., 2016, The end of the Ediacaran: Two new exceptionally preserved  
251 body fossil assemblages from Mount Dunfee, Nevada, USA: *Geology*, v. 44, p. 911–  
252 914, doi:10.1130/G38157.1.
- 253 Steiner, M., Li, G., Qian, Y., Zhu, M., and Erdtmann, B.-D., 2007, Neoproterozoic to  
254 Early Cambrian small shelly fossil assemblages and a revised biostratigraphic  
255 correlation of the Yangtze Platform (China): *Palaeogeography, Palaeoclimatology,*  
256 *Palaeoecology*, v. 254, p. 67–99, doi:10.1016/j.palaeo.2007.03.046.
- 257 Wood, R.A., Poulton, S.W., Prave, A.R., Hoffmann, K.-H., Clarkson, M.O., Guilbaud,  
258 R., Lyne, J.W., Tostevin, R., Bowyer, F., Penny, A.M., Curtis, A., and Kasemann,  
259 S.A., 2015, Dynamic redox conditions control late Ediacaran metazoan ecosystems  
260 in the Nama Group, Namibia: *Precambrian Research*, v. 261, p. 252–271,  
261 doi:10.1016/j.precamres.2015.02.004.
- 262 Wood, R., Zhuravlev, A.Yu., Sukhov, S.S., Zhu, M., and Zhao, F., 2016, Demise of  
263 Ediacaran dolomitic seas marks widespread biomineralisation on the Siberian  
264 platform: *Geology*, v. 45, p. 27–30, doi:10.1130/G38367.1.
- 265 Yang, B., Steiner, M., Zhu, M., Li, G., Liu, J., and Liu, P., 2016a, Transitional Ediacaran-  
266 Cambrian small skeletal fossil assemblages from South China and Kazakhstan:  
267 Implications for chronostratigraphy and metazoan evolution: *Precambrian Research*,  
268 v. 285, p. 202–215, doi:10.1016/j.precamres.2016.09.016.

- 269 Yang, C., Li, X.-H., Zhu, M., and Condon, D.J., 2016b, SIMS U-Pb zircon  
270 geochronological constraints on the upper Ediacaran stratigraphic correlations, South  
271 China: Geological Magazine, p. 1–15, doi:10.1017/S0016756816001102.
- 272 Zhu, M.Y., Li, G.X., Zhang, J.M., Steiner, M., Qian, Y., and Jiang, Z.W., 2001, Early  
273 Cambrian stratigraphy of east Yunnan, southwestern China: A synthesis: Acta  
274 Palaeontologica Sinica, v. 40, p. 4–39.
- 275 Zhu, M.-Y., Babcock, L.E., and Peng, S.-C., 2006, Advances in Cambrian stratigraphy  
276 and paleontology: Integrating correlation techniques, paleobiology, taphonomy and  
277 paleoenvironmental reconstruction: Palaeoworld, v. 15, p. 217–222,  
278 doi:10.1016/j.palwor.2006.10.016.
- 279 Zhu, M., Strauss, H., and Shields, G.A., 2007, From Snowball Earth to the Cambrian  
280 bioradiation: Calibration of Ediacaran-Cambrian Earth history in South China:  
281 Palaeogeography, Palaeoclimatology, Palaeoecology, v. 254, p. 1–6,  
282 doi:10.1016/j.palaeo.2007.03.026.
- 283 Zhuravlev, A. Yu., Gámez Vintaned, J.A., and Ivantsov, A. Yu., 2009, First finds of  
284 problematic Ediacaran fossil *Gaojiashania* in Siberia and its origin: Geological  
285 Magazine, v. 146, p. 775–780, doi:10.1017/S0016756809990185.
- 286 Zhuravlev, A.Yu., Liñán, E., Gámez Vintaned, J.A., Debrenne, F., and Fedorov, A.B.,  
287 2012, New finds of skeletal fossils in the terminal Neoproterozoic of the Siberian  
288 Platform and Spain: Acta Palaeontologica Polonica, v. 57, p. 205–224,  
289 doi:10.4202/app.2010.0074.

290

291 FIGURE CAPTIONS



292

293 Figure 1. The Yudoma Group, Kyra–Ytyga River section, Yudoma River, with inset map  
294 of the Siberian Platform, Russia. A: Map of the Siberian Platform showing structural-  
295 facies regions (modified after Khomentovsky, 2008; F1a – Uchur-Maya Plate and F1b –  
296 Yudoma-Maya Depression, F2 – Lena-Aldan, F3 – Baykal-Lena, F4 – Enisey-Angara,  
297 F5a – Igarka-Noril’sk Uplift, F5b – Anabar Uplift, and F5c – Olenek Uplift), the Yudoma  
298 River sections (1 – Kyra-Ytyga River, 2 – Nuuchchalakh valley, 3 – Yudoma-Maya  
299 confluence) and the well-investigated transitional Ediacaran-Cambrian sections (4 –  
300 Dvortsy, Aldan River, 5 – Olenek and Khorbusuonka rivers, 6 – Bol’shay and Malaya  
301 Kuonamka rivers, 7 – Sukharikha River). B: Stratigraphic log, carbon isotope  
302 chemostratigraphy, and fossil distribution. Levels I, II, III, IV and V mark the fossil  
303 horizons of the section.

304

305 Figure 2. Fossils from the Kyra-Ytyga River section. **A–C:** *Cloudina* ex gr. *C. riemkeae*,  
306 Level-II. **D:** cloudinid, Level-IV. **E:** cloudinid, Level-II. **F:** *A. valkovi*, Level-II. **G:**  
307 *Anabarites natellus*, Level-IV. **H:** *A. latus*, Level-IV. **I:** *Aculeochrea composita*, Level-  
308 IV. **J:** *Sachites* sp., Level-V. **K:** *Hyolithellus tenuis*, Level-V. **L:** *Protohertzina*  
309 *?anabarica*, Level-V. **M:** *P. unguiformis*, Level-IV. **N:** *Fomitchella acinaciformis*,  
310 Level-V. **O:** chancelloriid, Level-V. **P:** *Fomitchella infundibuliformis*, Level-V. **Q:**  
311 *Halkieria* sp., Level-V. **R:** undetermined shelly fossils, Level-II. **S:** anabaritid packstone,  
312 Level-III. **T:** 1, *Anabarites trisulcatus*, b, *A. latus*; Level-III. **U:** *Beltanelliformis brunsae*,  
313 Level-I. **V:** *Diplocraterion* sp., Level-V. **W:** *Shaanxilites* sp., from the Aim Formation at  
314 Nuuchchalakh valley. Photography: **A–R** – Aleksandr Fedorov, (**U**) – Andrey Ivantsov.

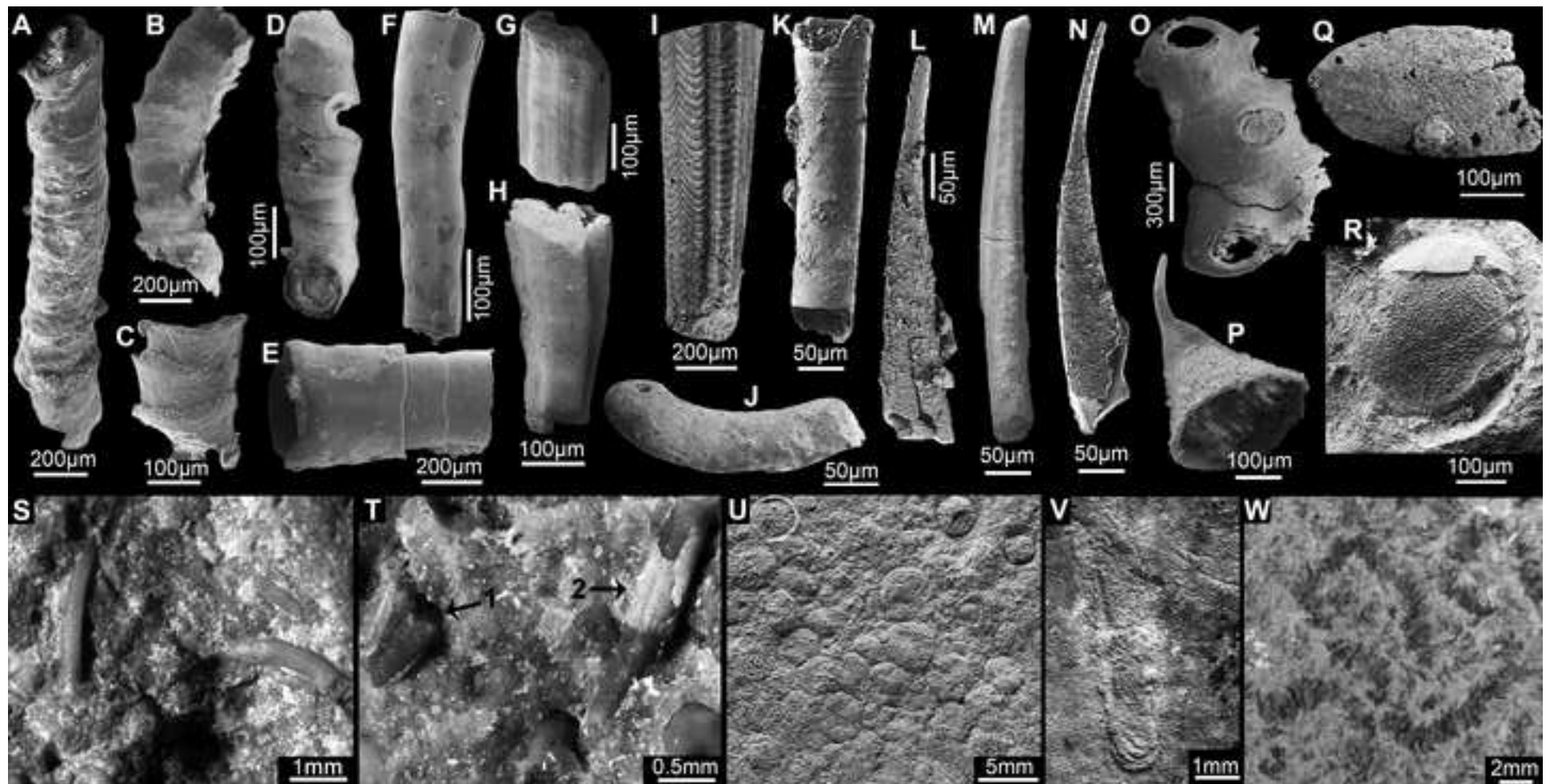
315

316 Figure 3. Summary of temporal distribution of the terminal Ediacaran soft-bodied fossils,  
317 Ediacaran to Cambrian skeletal fossils, together with general carbon isotope  
318 chemostratigraphy (modified after Zhu et al., 2006, 2007 with explanation of the  
319 acronyms for the isotope excursions DOUNCE/SHURAM, BASE, SHICE and ZHUCE)  
320 and the approximate duration of the Great Unconformity. Current categories of  
321 ‘Ediacaran-type (E-type)’ and ‘Cambrian-type’ skeletal fossils are shown, with  
322 established zones SSF I, II, and III, and the proposed *Cloudina-Namacalathus-*  
323 *Sinotubulites* Assemblage Zone (CNS Zone).

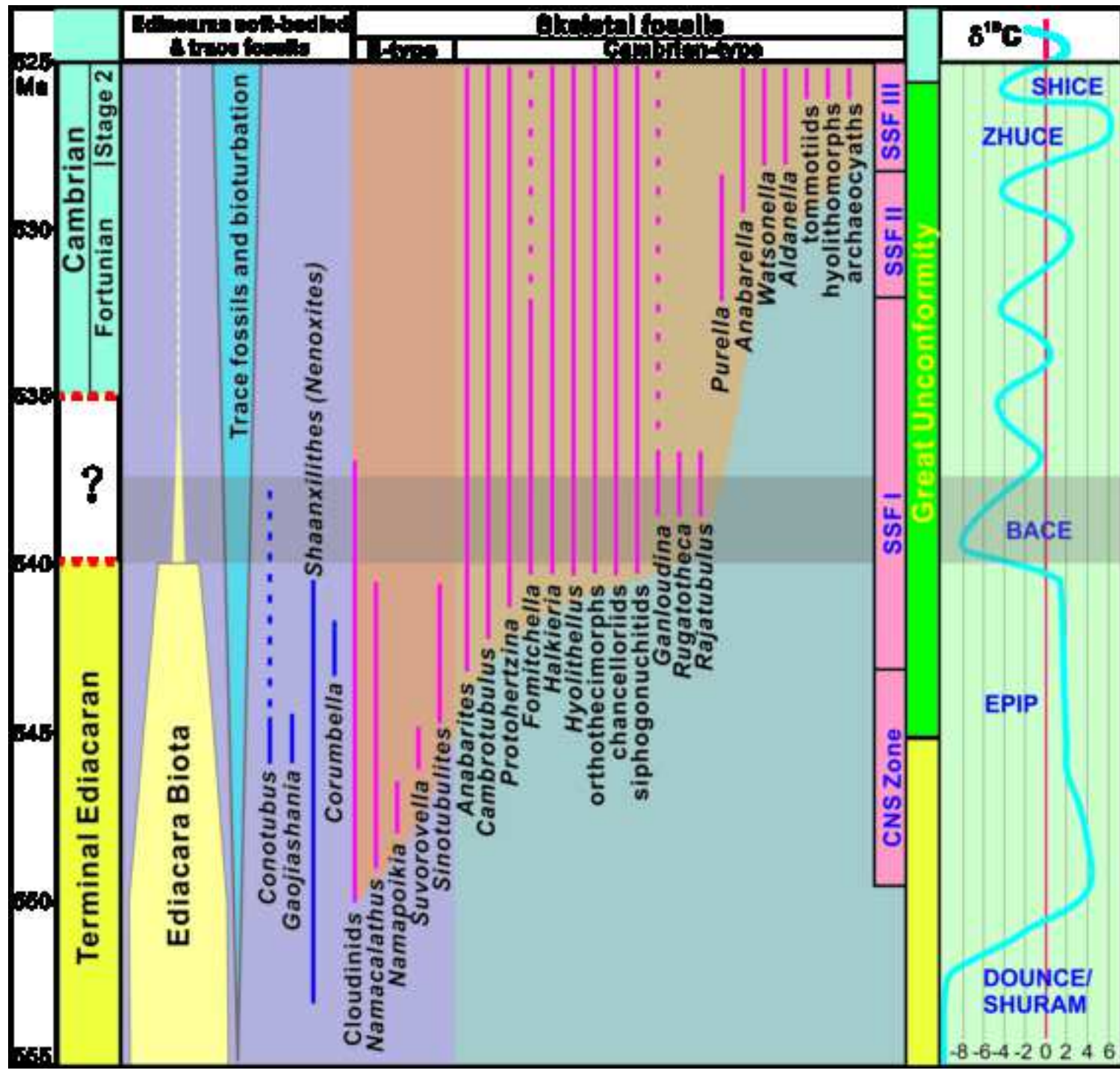
324

325 <sup>1</sup>GSA Data Repository item 2017xxx, xxxxxxxx, is available online at  
326 [www.geosociety.org/datarepository/2017](http://www.geosociety.org/datarepository/2017) or on request from [editing@geosociety.org](mailto:editing@geosociety.org).









## Supplementary Materials

1  
2  
3  
4  
5  
6  
7  
8  
9  
10  
11  
12  
13  
14  
15  
16  
17  
18  
19  
20  
21  
22  
23  
24  
25  
26

### Locality information

Kyra-Ytyga river = 59°29'38.7"N 137°14'41.0"E

### List of fossils of the Yudoma Group from sections on the Yudoma River, south-eastern

#### Siberian Platform (Republic of Sakha (Yakutia), Russia)

#### Level I. Aim Formation

##### 1. Kyra-Ytyga River section:

- *Beltanelliformis brunsa* Menner in Keller et al., 1974 – moulds on limy siltstone bedding surfaces, 30.0-45.0 m above the base of the formation, collection A. Ivantsov and A. Zhuravlev, 1998 (?*Nemiana simplex* in Ivantsov et al., 2014, fig. 5; Ivantsov, 2017; Fig. 2U, herein).
- ?*Shaanxilithes* sp. – imprints on limy siltstone bedding surfaces, 29.5-45.0 m above the base of the formation, collection A. Zhuravlev et al., 2015 (Wood et al., 2016).

##### 2. Nuuchchalakh valley section:

- *Shaanxilithes* sp. (= *Nenoxites* sp.) – imprints on limy siltstone bedding surfaces of black limestone, 80.4-94.5 m above the base of the formation, collection A. Ivantsov and A. Zhuravlev, 1998 (*Gaojiashania annulocosta* in Zhuravlev et al., 2009, fig. 2; *Shaanxilithes* in Cai et al., 2011; *Gaojiashania* in Wood et al., 2016, fig. 2A; *Nenoxites curvus* in Ivantsov, 2017, fig. 2r; Fig. 2W herein).
- Acritarchs *Leiomarginatasphaera punctulata* Pyatiletov, 1988; *Granomarginatasphaera judomica* Pyatiletov, 1988; *Bailikania diligena* Treshchetenkova, 1981; “*Sibiriella*” *prima* Fayzulina, 1981; *Bavlinella faveolata* (Shepeleva, 1963) Vidal, 1976; *Leiovalia*

27 sp.; *Leiosphaeridia rubiginosa* (Andreeva, 1966) Jankauskas et al., 1989; *L.*  
28 *minutissima* (Naumova, 1949) Jankauskas et al. 1989; *L. minuta* (Naumova, 1961)  
29 Jankauskas et al., 1989; *Siphonophycus robustum* (Schopf, 1968) Knoll et al., 1991; *S.*  
30 *typicum* (Hermann, 1974) Butterfield et al., 1994 – organic envelopes from black  
31 siltstone, 11.6-27.6 m above the base of the formation (Pyatiletov, 1988, pls. 1, 2; names  
32 are corrected in accordance with current systematics).

33

34

### 35 3. **Yudoma-Maya confluence section:**

- 36 ● *Beltanelliformis brunsaе* Menner in Keller et al., 1974 – moulds on bedding surfaces of  
37 black sandstone, 11.0-11.3 m above the base of the section, collections A. Ivantsov,  
38 2014; A. Ivantsov and A. Zhuravlev, 2015 (Ivantsov, 2017, fig.2a).
- 39 ● *Palaeopascichnus* sp. – moulds on bedding surfaces of black sandstone, 11.0-11.3 m  
40 above the base of the section, collections A. Ivantsov, 2014; A. Ivantsov and A.  
41 Zhuravlev, 2015 (Ivantsov, 2017, fig. 2B).
- 42 ● *Aspidella terranovica* Billings, 1872 – moulds on bedding surfaces of black sandstone,  
43 11.0-11.3 m above the base of the section, collections A. Ivantsov, 2014; A. Ivantsov  
44 and A. Zhuravlev, 2015 (Wood et al., 2016, fig. 2E; Ivantsov, 2017, fig. 2G).
- 45 ● *Suvorovella aldanica* Vologdin and Maslov, 1960 – complete and fragmented shells in  
46 dolomitic shelly packstone, 14.6-16.9 m above the base of the section, collections A.  
47 Ivantsov, 2014; A. Ivantsov and A. Zhuravlev, 2015 (*Suvorovella aldanica*, *Majaella*  
48 *verkhojanica*, *Majaella* sp. I, and *Hyalolithoides* in Vologdin and Maslov, 1960, fig. 1;  
49 *Suvorovella aldanica* and *Cyclomedusa* sp. in Sokolov, 1972, figs. 5, 6; *Suvorovella* sp.  
50 and *Cyclomedusa* ex. gr. *plana* in Sokolov, 1976, figs. a, r; Ivantsov, 2016; Wood et al.,  
51 2016, fig. 2C).

52

53 **Level II. Ust'-Yudoma Formation, 183 m above the base**

54 **Kyra-Ytyga River section:**

- 55 ● *Cloudina* ex gr. *C. riemkeae* Germs, 1972 – phosphatized tubes from limy dolomitic  
56 packstone, collection A. Fedorov, 1981 (Zhuravlev et al., 2012, fig. 3A-E; Wood et al.,  
57 2016, fig. 2E; Fig. 2A-C, herein).
- 58 ● Cloudinids – phosphatized tubes from limy dolomitic packstone, collection A. Fedorov,  
59 1981 (Fig. 2E, herein).
- 60 ● *Anabarites trisulcatus* Missarzhevsky in Voronova and Missarzhevsky, 1969 –  
61 phosphatized steinkerns from limy dolomitic packstone, collection A. Fedorov, 1981  
62 (Wood et al., 2016, fig. 2F).
- 63 ● *A. valkovi* (Bokova in Bokova and Vasil'eva, 1990) – phosphatized steinkerns from limy  
64 dolomitic packstone, collection A. Fedorov, 1981 (Fig. 2F, herein).
- 65 ● Spaeroid shelly problematica – shells from limy dolomitic packstone, collection A.  
66 Fedorov, 1981 (Fig. 2R, herein).
- 67 ● Megasphaeromorph acritarchs – dolomitized envelopes from dolomitic packstone,  
68 collection A. Fedorov, 1981 (Wood et al., 2016, fig. 2D).

69

70 **Level III. Ust'-Yudoma Formation, 260 m above the base**

71 **Kyra-Ytyga River section:**

- 72 ● *Anabarites trisulcatus* Missarzhevsky in Voronova and Missarzhevsky, 1969 – shells  
73 and steinkerns from limy dolomitic packstone, collection A. Zhuravlev et al., 2015 (Fig.  
74 2T1, herein).
- 75 ● *A. latus* (Vail'kov and Sysoev, 1970) – shells and steinkerns from limy dolomitic  
76 packstone, collection A. Zhuravlev et al., 2015 (Fig. 2T2, herein).
- 77 ● *A. hexsulcatus* Missarzhevsky, 1974 – shells and steinkerns from limy dolomitic  
78 packstone, collection A. Zhuravlev et al., 2015.



79 ● *Cambrotubulus decurvatus* Missarzhevsky in Rozanov et al., 1969 – shells and  
80 steinkerns from limy dolomitic packstone, collection A. Zhuravlev et al., 2015 (Fig. 2S,  
81 herein).

82

83 **Level IV. Ust'-Yudoma Formation, 8 m below the top**

84 **Kyra-Ytyga River section:**

85 ● *Anabarites trisulcatus* Missarzhevsky in Voronova and Missarzhevsky, 1969 –  
86 phosphatized steinkerns from limy dolomitic packstone, collection Yu. Shabanov, 1967.

87 ● *A. latus* (Vail'kov and Sysoev, 1970) – phosphatized steinkerns from limy dolomitic  
88 packstone, collection Yu. Shabanov, 1967 (Fig. 2H, herein).

89 ● *A. natellus* (Vail'kov and Sysoev, 1970) – phosphatized steinkerns from limy dolomitic  
90 packstone, collection Yu. Shabanov, 1967 (Fig. 2G, herein).

91 ● *A. tripartitus* Missarzhevsky in Rozanov et al., 1969 – phosphatized steinkerns from  
92 limy dolomitic packstone, collection Yu. Shabanov, 1967.

93 ● *Aculeochrea composita* (Missarzhevsky in Rozanov et al., 1969) – phosphatized  
94 steinkerns from limy dolomitic packstone, collection Yu. Shabanov, 1967 (Fig. 2I,  
95 herein).

96 ● *Cambrotubulus decurvatus* Missarzhevsky in Rozanov et al., 1969 – phosphatized  
97 steinkerns from limy dolomitic packstone, collection Yu. Shabanov, 1967.

98 ● Cloudinids – phosphatized tubes from limy dolomitic packstone, collection Yu.  
99 Shabanov, 1967 (Fig. 2D, herein).

100 ● *Protohertzina unguiformis* Missarzhevsky, 1973 – phosphatic shells from limy  
101 dolomitic packstone, collection Yu. Shabanov, 1967 (Fig. 2M, herein).

102

103

104

105 **Level V. Ust'-Yudoma Formation, 4.7 m below the top**

106 **Kyra-Ytyga River section:**

- 107 ● *Anabarites trisulcatus* Missarzhevsky in Voronova and Missarzhevsky, 1969 –  
108 phosphatized steinkerns from limy dolomitic packstone, collection Yu. Shabanov, 1967.
- 109 ● *Cambrotubulus decurvatus* Missarzhevsky in Rozanov et al., 1969 – phosphatized  
110 steinkerns from limy dolomitic packstone, collection Yu. Shabanov, 1967.
- 111 ● *Protohertzina ?anabarica* Missarzhevsky, 1973 – phosphatic shells from limy dolomitic  
112 packstone, collection Yu. Shabanov, 1967 (Fig. 2L, herein).
- 113 ● *Fomitchella acinaciformis* Missarzhevsky in Rozanov et al., 1969 – phosphatic shells  
114 from limy dolomitic packstone, collection Yu. Shabanov, 1967 (Fig. 2N, herein).
- 115 ● *F. infundibuliformis* Missarzhevsky in Rozanov et al., 1969 – phosphatic shells from  
116 limy dolomitic packstone, collection Yu. Shabanov, 1967 (Fig. 2P, herein).
- 117 ● *Halkieria* sp. – phosphatized steinkerns from limy dolomitic packstone, collection Yu.  
118 Shabanov, 1967 (Fig. 2Q, herein).
- 119 ● *Sachites* sp. – phosphatized steinkerns from limy dolomitic packstone, collection Yu.  
120 Shabanov, 1967 (Fig. 2J, herein).
- 121 ● Chancelloriid – phosphatized steinkern from limy dolomitic packstone, collection V.  
122 Khomentovsky, 1967 (Fig. 2O, herein).
- 123 ● *Hyolithellus tenuis* Missarzhevsky in Rozanov and Missarzhevsky, 1966 – phosphatic  
124 tubes from limy dolomitic packstone, collection Yu. Shabanov, 1967 (Fig. 2K, herein).
- 125 ● Siphogonuchitid – phosphatized steinkern from limy dolomitic packstone, collection Yu.  
126 Shabanov, 1967.
- 127 ● *Allathea* sp. – calcareous shells from limy dolomitic packstone, collection A.  
128 Zhuravlev et al., 2015.
- 129 ● *Diplocraterion* sp. – vertical burrowing trace fossil from limy dolomitic packstone,  
130 collection A. Zhuravlev et al., 2015 (Fig. 2V, herein).

131

132 **REFERENCES CITED**

- 133 Cai, Y., Hua, H., Zhuravlev, A.Yu., Gámez Vintaned, J.A., and Ivantsov, A. Yu., 2011, Discussion  
134 of 'First finds of problematic Ediacaran fossil *Gaojiashania* in Siberia and its origin':  
135 Geological Magazine, v. 148, p. 329–333, doi:10.1017/S0016756810000749.
- 136 Ivantsov, A.Yu., 2017, On the finds of typical Ediacaran fossils in the Vendian Yudoma Group of  
137 eastern Siberia: Doklady Akademii nauk, v. 472, p. 1–4 [in Russian].
- 138 Ivantsov, A.Yu., Gritsenko, V.P., Konstantinenko, L.I., and Zakrevskaya, M.A., 2014, Revision of  
139 the problematic macrofossil *Beltanelliformis* (= *Beltanella*, *Nemiana*): Paleontological Journal,  
140 v. 48, p. 1423–1448, doi: 10.1134/S0031030114130036.
- 141 Pyatiletov, V.G., 1988, Late Precambrian microfossils of the Uchur-Maya Region, in  
142 Khomentovsky, V.V., and Shenfil', V.Yu., eds., Late Precambrian and Early Palaeozoic of  
143 Siberia, Riphean and Vendian, Collection of Scientific Papers: Institute of Geology and  
144 Geophysics, Siberian Branch, USSR Academy of Sciences, Novosibirsk, p. 47–104 [in  
145 Russian].
- 146 Sokolov, B.S., 1972, The Vendian Stage in the Earth history, in International Geological Congress,  
147 27<sup>th</sup> Session, Reports of Soviet Geologists, Problem 7, Paleontology: Nauka, Moscow, p. 114-  
148 124 [in Russian].
- 149 Sokolov, B.S., 1976, Organic world on the Earth at the approach of the Phanerozoic differentiation:  
150 Vestnik Akademii nauk SSSR, v. 1, p. 126–143 [in Russian].
- 151 Vologdin, A.G., and Maslov, A.B., 1960, On a new group of fossil organisms from the lower  
152 Yudoma Formation of the Siberian Platform: Doklady Akademii nauk SSSR, v. 134, p. 691–  
153 693 [in Russian].
- 154 Wood, R. Zhuravlev, A.Yu., Sukhov, S.S., Zhu, M., and Zhao, F., 2016, Demise of Ediacaran  
155 dolomitic seas marks widespread biomineralisation on the Siberian platform: Geology,  
156 doi:10.1130/G38367.1.

157 Zhuravlev, A.Yu., Gámez Vintaned, J.A., and Ivantsov, A. Yu., 2009, First finds of  
158 problematic Ediacaran fossil *Gaojiashania* in Siberia and its origin: Geological Magazine,  
159 v. 146, p. 775–780, doi:10.1017/S0016756809990185.

160 Zhuravlev, A.Yu., Liñán, E., Gámez Vintaned, J.A., Debrenne, F., and Fedorov, A.B., 2012, New  
161 finds of skeletal fossils in the terminal Neoproterozoic of the Siberian Platform and Spain: Acta  
162 Palaeontologica Polonica, v. 57, p. 205–224, doi:10.4202/app.2010.0074.

163

164

165 **Carbon and Oxygen isotope data of the Kyra-Ytyga section**

166 Stratigraphic height (m) of samples starts from the first carbonate at the middle of the Aim  
 167 Formation of the section. Microdrilling samples of carefully selected micritic carbonate were  
 168 analysed for  $\delta^{13}\text{C}$  and  $\delta^{18}\text{O}$  data simultaneously by a Thermo Scientific MAT-253 mass  
 169 spectrometer with Kiel IV Carbonate Device at the State Key Laboratory of Palaeobiology and  
 170 Stratigraphy, Nanjing Institute of Geology and Palaeontology, Chinese Academy of Sciences.  
 171 Carbonate  $\delta^{13}\text{C}$  and  $\delta^{18}\text{O}$  isotopic results are reported in per mil (‰) notation relative to VPDB  
 172 (Vienna Peedee belemnite). Standard deviation is better than 0.03 ‰ for  $\delta^{13}\text{C}$  and 0.08 ‰ for  $\delta^{18}\text{O}$   
 173 based on the national standard (Reference number GBW 04405).

174

Samples	Height(m)	$\delta^{13}\text{C}_{\text{PDB}}$	$\delta^{18}\text{O}_{\text{PDB}}$
KY0	0	1.137	-6.369
KY0.2	0.2	1.091	-6.045
KY0.5	0.5	1.184	-6.332
KY0.8	0.8	0.170	-7.666
KY1	1	1.234	-5.168
KY1.5	1.5	0.915	-7.800
KY1.9	1.9	1.074	-7.794
KY2.55	2.55	1.373	-1.221
KY2.8	2.8	1.094	-7.041
KY3.5	3.5	1.004	-3.844
KY4	4	1.191	-9.719
KY4.6	4.6	1.203	-4.623
KY5	5	1.290	-8.882
KY5.8	5.8	1.605	-8.349
KY6.5	6.5	0.848	-10.900
KY7.6	7.6	0.029	-7.663
KY8.5	8.5	0.069	-7.651
KY9	9	-0.102	-8.032
KY9.1	9.1	-0.269	-9.557
KY9.4	9.4	-0.418	-9.793
KY9.5	9.5	-0.753	-9.333
KY15	15	2.977	-7.958
KY15.4	15.4	3.407	-8.092
KY16	16	3.732	-6.826
KY16.5	16.5	3.676	-7.169
KY17	17	3.095	-7.436
KY21	21	0.984	-7.764
KY21.4	21.4	1.650	-7.290
KY21.9	21.9	1.780	-7.143
KY22.1	22.1	0.975	-7.084
KY22.4	22.4	1.307	-6.768
KY23	23	2.416	-7.162
KY23.7	23.7	3.308	-6.817
KY24.2	24.2	3.319	-6.946
KY29.7	29.7	3.801	-5.801

KY30	30	3.502	-6.705
KY31	31	3.710	-5.502
KY31.3	31.3	3.784	-6.222
KY31.4	31.4	3.812	-6.231
KY31.9	31.9	3.950	-5.631
KY33.1	33.1	3.806	-5.731
KY34	34	2.871	-6.407
KY34.3	34.3	2.091	-5.949
KY35	35	3.207	-5.444
KY37.5	37.5	2.685	-6.066
KY37.7	37.7	2.676	-5.833
KY37.8	37.8	2.763	-5.848
KY38	38	2.357	-6.047
KY38.5	38.5	2.488	-5.770
KY39	39	2.577	-5.859
KY48	48	0.556	-6.054
KY48.3	48.3	-0.515	-5.553
KY48.8	48.8	1.162	-7.308
KY49.3	49.3	0.728	-6.504
KY49.9	49.9	0.993	-6.398
KY50	50	1.859	-6.881
KY51	51	0.040	-6.929
KY51.3	51.3	-0.575	-6.875
KY51.8	51.8	-1.273	-7.025
KY52	52	1.202	-7.107
KY52.1	52.1	-0.696	-6.963
KY52.2	52.2	0.106	-6.000
KY52.5	52.5	1.184	-7.416
KY53.3	53.3	0.872	-7.223
KY53.7	53.7	0.728	-7.560
KY54.1	54.1	1.631	-7.726
KY54.5	54.5	1.921	-9.493
KY54.7	54.7	2.342	-10.080
KY55	55	1.570	-12.756
KY55.4	55.4	1.651	-11.929
KY55.5	55.5	1.157	-8.730
KY55.9	55.9	1.086	-7.395
KY56	56	1.443	-7.950
KY56.4	56.4	1.673	-6.645
KY57.3	57.3	2.639	-10.949
KY58.1	58.1	2.741	-9.906
KY59.1	59.1	2.322	-7.898
KY59.9	59.9	2.838	-10.053
KY61	61	2.764	-11.199
KY62	62	1.382	-10.798
KY63.2	63.2	1.318	-9.710
KY64.4	64.4	1.995	-8.463
KY66	66	1.779	-8.193
KY67	67	1.743	-8.103
KY68	68	1.829	-7.987
KY69	69	1.931	-8.265
KY70	70	1.910	-7.794
KY71	71	2.013	-8.976
KY72	72	2.017	-8.097
KY73	73	2.135	-7.925
KY74	74	2.347	-9.267
KY75	75	2.338	-9.916

KY76	76	2.571	-8.943
KY77	77	2.837	-8.496
KY78	78	2.556	-10.992
KY79	79	1.990	-10.268
KY80	80	2.625	-10.173
KY81	81	2.723	-9.483
KY82	82	2.456	-10.313
KY83	83	2.114	-11.158
KY84	84	2.155	-10.755
KY85	85	2.647	-10.633
KY86	86	2.440	-9.984
KY87	87	2.026	-10.901
KY88	88	2.286	-11.028
KY89	89	2.453	-10.648
KY91	91	2.606	-9.757
KY92	92	2.691	-9.790
KY93	93	2.220	-9.599
KY94	94	2.453	-10.004
KY95	95	2.852	-10.228
KY96	96	2.914	-8.630
KY97	97	2.818	-6.648
KY98	98	2.809	-7.909
KY99	99	2.748	-8.467
KY100	100	2.629	-9.076
KY101	101	2.770	-9.423
KY102	102	2.844	-8.316
KY103	103	2.848	-9.009
KY104	104	2.486	-7.816
KY105	105	2.948	-9.882
KY106	106	2.623	-10.360
KY107	107	2.767	-9.917
KY109	109	2.816	-8.522
KY111	111	2.097	-10.026
KY113	113	2.786	-7.860
KY114	114	2.772	-8.669
KY115	115	2.736	-7.528
KY116	116	3.038	-6.324
KY117	117	2.781	-8.326
KY118	118	2.657	-7.678
KY119	119	2.362	-9.012
KY120	120	2.224	-7.461
KY121	121	2.965	-7.214
KY122	122	2.922	-6.366
KY123	123	2.987	-7.306
KY124	124	2.851	-8.823
KY125	125	2.916	-7.066
KY126	126	2.833	-7.536
KY127	127	2.395	-7.909
KY128	128	2.819	-7.198
KY129	129	2.690	-6.209
KY130	130	2.912	-4.790
KY131	131	3.001	-6.193
KY132	132	2.727	-6.717
KY133	133	2.982	-5.625
KY134	134	2.731	-8.529
KY135	135	3.175	-8.564
KY136	136	3.111	-4.380

KY137	137	2.980	-6.832
KY138	138	2.706	-8.058
KY139	139	2.529	-8.296
KY140	140	2.962	-5.458
KY141	141	2.965	-5.081
KY142	142	2.916	-4.209
KY143	143	2.210	-7.396
KY144	144	2.729	-6.486
KY145	145	2.691	-8.539
KY146	146	2.805	-9.121
KY147	147	2.331	-10.239
KY147.3	147.3	2.838	-9.399
KY148	148	2.876	-8.886
KY149	149	2.820	-8.283
KY150	150	2.552	-8.013
KY151	151	2.701	-7.294
KY152	152	2.700	-7.538
KY153	153	2.646	-7.650
KY154	154	2.094	-7.351
KY155	155	2.363	-7.876
KY156	156	2.296	-8.653
KY157	157	1.683	-7.953
KY158	158	2.005	-7.703
KY159	159	1.707	-7.154
KY161.5	161.5	3.021	-7.808
KY162	162	2.695	-8.225
KY163	163	2.953	-9.694
KY164	164	2.842	-6.932
KY165	165	2.459	-8.928
KY166	166	2.327	-9.921
KY167	167	1.938	-9.473
KY168	168	2.541	-9.154
KY169	169	2.261	-9.095
KY170	170	2.912	-8.100
KY171	171	2.896	-7.613
KY172	172	2.594	-8.586
KY173	173	2.886	-7.686
KY174	174	2.379	-8.475
KY175	175	2.596	-8.777
KY176	176	2.777	-7.994
KY177	177	1.335	-9.373
KY178	178	2.549	-8.931
KY179	179	2.133	-8.519
KY180	180	2.603	-7.439
KY181	181	1.856	-8.763
KY182	182	1.906	-7.637
KY183	183	1.674	-9.969
KY184	184	2.443	-7.003
KY185	185	2.103	-6.402
KY186	186	2.300	-6.394
KY187	187	1.514	-8.500
KY188	188	2.403	-7.670
KY189	189	2.441	-9.263
KY190	190	2.082	-9.511
KY191	191	2.733	-9.540
KY192	192	2.850	-9.645
KY192.8	192.8	2.783	-10.085



KY194	194	2.226	-9.953
KY195	195	2.548	-9.760
KY196	196	2.658	-10.785
KY197	197	2.475	-9.762
KY198	198	1.827	-9.621
KY199	199	2.045	-9.681
KY200	200	2.115	-8.269
KY201	201	2.223	-8.623
KY202	202	1.918	-9.472
KY203	203	2.027	-9.136
KY204	204	2.260	-9.757
KY205	205	0.943	-11.925
KY207	207	2.568	-9.015
KY208	208	2.327	-9.429
KY209	209	2.345	-9.959
KY210	210	2.167	-10.243
KY211	211	1.807	-10.626
KY213	213	1.593	-10.487
KY214.3	214.3	2.335	-9.735
KY215	215	2.198	-11.411
KY216	216	1.615	-11.246
KY217	217	1.862	-10.155
KY218	218	2.119	-9.736
KY219	219	1.485	-11.161
KY220	220	2.989	-8.741
KY221	221	1.343	-11.417
KY224	224	2.459	-11.075
KY225	225	1.496	-11.012
KY226	226	1.901	-9.857
KY227	227	1.987	-9.269
KY228	228	1.126	-11.993
KY228.8	228.8	2.022	-10.259
KY230	230	1.849	-9.322
KY231	231	0.945	-12.062
KY232	232	2.513	-9.533
KY233	233	2.258	-11.619
KY234	234	1.336	-11.080
KY235	235	0.956	-12.130
KY236	236	2.379	-9.474
KY237	237	1.933	-11.322
KY238	238	0.871	-10.762
KY239	239	2.154	-5.096
KY240	240	0.181	-12.179
KY241	241	1.813	-9.056
KY242	242	2.051	-9.798
KY243	243	2.064	-10.238
KY244	244	0.726	-11.169
KY245	245	2.423	-9.716
KY247	247	2.722	-8.893
KY248	248	0.727	-11.899
KY249	249	2.195	-10.415
KY250	250	0.954	-12.015
KY251	251	2.032	-8.886
KY252	252	1.306	-10.497
KY253	253	1.149	-11.372
KY255	255	1.234	-10.766
KY256	256	2.137	-9.856

KY257	257	0.798	-11.119
KY258	258	1.097	-11.314
KY259	259	1.604	-9.842
KY260	260	1.633	-9.469
KY261	261	1.388	-9.913
KY262	262	2.153	-9.823
KY263	263	2.219	-10.537
KY264	264	2.608	-8.424
KY265	265	2.452	-10.003
KY266	266	2.419	-9.472
KY267.5	267.5	2.477	-9.880
KY269	269	0.871	-10.712
KY270	270	2.016	-9.037
KY271	271	1.634	-9.074
KY272	272	1.179	-11.426
KY272.5	272.5	0.671	-8.526
KY274	274	2.371	-8.918
KY275	275	2.066	-8.286
KY276	276	1.843	-10.199
KY277	277	0.944	-8.978
KY278	278	1.795	-8.299
KY279	279	1.771	-8.308
KY280	280	1.367	-8.231
KY281	281	0.748	-8.725
KY282	282	0.556	-8.798
KY283	283	0.686	-8.107
KY284	284	1.655	-8.395
KY285	285	1.527	-8.333
KY287	287	1.229	-8.608
KY288	288	0.844	-8.861
KY289	289	0.720	-8.663
KY290	290	1.119	-9.228
KY291	291	0.434	-8.058
KY292	292	0.476	-8.179
KY293	293	1.357	-7.354
KY294	294	0.422	-11.762
KY295.5	295.5	0.337	-7.685
KY301	301	0.398	-9.192
KY302.3	302.3	0.354	-8.066
KY303	303	0.651	-8.962
KY311	311	1.709	-8.015
KY312	312	1.291	-7.967
KY312.5	312.5	1.386	-7.699
KY313	313	1.085	-6.871
KY313.6	313.6	0.845	-8.064
KY314	314	0.951	-8.515
KY314.5	314.5	1.166	-7.681
KY315	315	1.070	-6.851
KY315.5	315.5	1.431	-8.036
KY316	316	0.901	-7.757
KY316.5	316.5	0.852	-8.364
KY317	317	0.928	-7.287
KY317.5	317.5	0.519	-8.322
KY318	318	0.552	-7.752
KY318.5	318.5	0.509	-8.702
KY319	319	0.638	-9.048
KY319.5	319.5	0.600	-7.409

KY320	320	0.494	-6.904
KY320.5	320.5	0.816	-8.396
KY321	321	0.788	-7.344
KY321.5	321.5	0.149	-9.965
KY322	322	0.357	-8.989
KY322.5	322.5	0.099	-8.718
KY323	323	0.891	-7.903
KY323.5	323.5	0.401	-7.187
KY324	324	0.180	-7.800
KY325	325	0.145	-7.350
KY325.5	325.5	0.171	-7.962
KY325.8	325.8	0.464	-7.549
KY326	326	0.254	-7.770
KY326.5	326.5	0.035	-8.580
KY327	327	0.051	-8.987
KY327.5	327.5	0.302	-7.810
KY328	328	0.289	-7.873
KY328.5	328.5	0.470	-8.544
KY329	329	0.017	-7.809
KY329.5	329.5	0.307	-7.736
KY330	330	0.138	-7.716
KY330.5	330.5	-0.092	-7.960
KY331	331	-0.011	-8.056
KY331.5	331.5	0.006	-8.104
KY332	332	-0.237	-8.855
KY332.5	332.5	0.064	-8.252
KY333	333	0.027	-7.425
KY333.5	333.5	-0.105	-9.362
KY334	334	-0.605	-10.148
KY334.5	334.5	-0.335	-8.061
KY335	335	-0.650	-7.599
KY335.5	335.5	-0.622	-8.774
KY336	336	-0.620	-7.435